

## INFRARED SPECKLE METHODS

A.Chelli

Observatoire de Lyon - Av.Charles André 69230 ST GENIS LAVAL

I-INTRODUCTION The speckle interferometry method has been introduced in 1970 by A. Labeyrie who showed in the visible domain that it was possible to reach the limiting spatial resolution of large telescopes. From 1977, the method is extended to the near infrared between 2 and  $5\mu\text{m}$  (Léna, 1977; Wade and Selby, 1978), 7 years later infrared speckle systems are operating on several large telescopes (ESO, KPNO, AAT, UKIRT, CFHT ...).

The speckle interferometry method has allowed to better understanding the optical properties of the atmosphere, especially owing to the work of F.Roddier (Roddier, 1981). It has raised new problems like the phase restitution of the object spectrum and has largely contributed to the development of image reconstruction methods.

From the astrophysical point of view, spatial resolutions of  $0''.02$  to  $0''.2 - 0.5$  to  $5\mu\text{m}$  - have had considerable consequences :

In the visible domain one can mention applications in planetary (asteroids, Pluto-Charon system), solar (granulation), stellar (atmosphere) and extragalactic physics (quasar, nuclei of galaxies) and in astronomy (resolution of a few hundred of double systems).

In the infrared domain between 2 and  $5\mu\text{m}$  the speckle interferometry method is well suited to the study of circumstellar envelopes (cool giant and supergiants, OH/IR sources, very young objects ...) or to the discovery of infrared companions (T Tauri), extragalactic applications are possible (NGC 1068), but remain marginal up-to-now.

II-BASIC EQUATIONS Let  $\alpha$  be an angular variable on the sky,  $O_\lambda(\alpha)$  the monochromatic distribution of intensity in the object and  $I_\lambda(\alpha)$  the same quantity in the image given by a telescope. In the isoplanatic domain there is a convolution relation between  $I_\lambda(\alpha)$  and  $O_\lambda(\alpha)$ .

$$I_\lambda(\alpha) = O_\lambda(\alpha) * S_\lambda(\alpha)$$

where  $S_\lambda(\alpha)$  is the impulse response of the telescope plus atmosphere at the wavelength  $\lambda$  (in the following we shall omit the index  $\lambda$  for all the wavelength

*Proceedings of the IAU Colloquium No. 79: "Very Large Telescopes, their Instrumentation and Programs", Garching, April 9-12, 1984.*

dependent quantities).

In the Fourier space the last relation becomes

$$\tilde{I}(u) = \tilde{O}(u) \cdot \tilde{S}(u)$$

where  $u$  is a spatial frequency;  $\tilde{O}(u)$ ,  $\tilde{I}(u)$  and  $\tilde{S}(u)$  are respectively the object spectrum, the image spectrum and the transfer function.

1. Long exposure images. The properties of the long exposure images have been described by Hufnagel and Stanley (1964) and Fried (1965). The long exposure transfer function  $\langle \tilde{S}(u) \rangle_t$  (Fried, 1966) has the very simple form

$$\langle \tilde{S}(u) \rangle_t = B(u) T(u) \quad \text{with } B(u) = \exp \left\{ -3.44 \left( \frac{\lambda u}{r_0} \right)^{5/3} \right\}$$

where  $T(u)$  is the transfer function of the telescope without atmosphere -  $T(u)$  is zero at the cut-off frequency  $u_c = D/\lambda$  -; and  $B(u)$  is a term introduced by the atmospheric turbulence, depending on the Fried parameter  $r_0$ . It is clear that in the case of long exposure images the spatial resolution will be limited by the diameter  $D$  of the telescope if  $D < r_0$  and the by the atmospheric turbulence if  $D > r_0$ . In the visible and the near infrared ( $\lambda < 5 \mu\text{m}$ ), the typical values of  $r_0$  being respectively of the order of 10 and 100cm (see Roddier and Léna, 1984, for a detailed discussion), the resolution of large telescopes ( $D \gtrsim 400 \text{ cm}$ ) will be limited by the atmosphere.

2. Short exposure images. If we look at the "instantaneous" image of a point source given by a large telescope, we can see speckles located inside the seeing disk, the average size of the speckles being of the order of the size of the Airy disk given by the telescope alone. Labeyrie has proposed in 1970 to retain the high frequency information contained in the speckles by doing a statistical analysis on the power spectrum  $\langle |\tilde{I}(u)|^2 \rangle$  of a large number of short exposure images. The latter is given by

$$\langle |\tilde{I}(u)|^2 \rangle = |\tilde{O}(u)|^2 \cdot \langle |\tilde{S}(u)|^2 \rangle$$

where  $\langle |\tilde{S}(u)|^2 \rangle$  is the speckle transfer function, the brackets indicating an ensemble average. Korff et al. (1972) have shown that  $\langle |\tilde{S}(u)|^2 \rangle$  is non zero up to the telescope cut-off frequency, at high frequencies  $u \gg u_0 (=r_0/\lambda)$ ,

$$\langle |\tilde{S}(u)|^2 \rangle \sim \frac{T(u)}{N_s} \quad \text{with } N_s \sim 2.3 (D/r_0)^2$$

where  $N_s$  is the number of speckles in the image.

Two models have been proposed to describe the speckle transfer function. They suppose that the complex amplitude of the incident wave on the telescope pupil has either a log-normal statistics (Korff, 1973), or a normal statistics (Dainty, 1973). It seems that, at least in some cases, the complex amplitude

is well described by the log-normal model (Aime et al., 1979; Chelli et al., 1979; see figure 1).

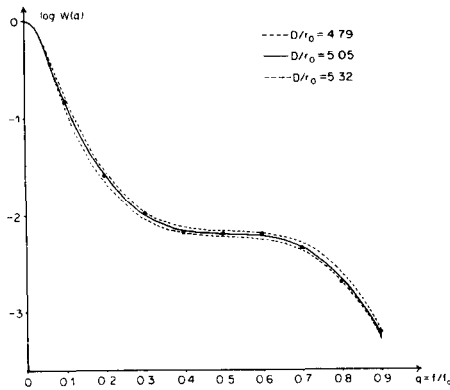


Fig.1. Speckle transfer function. The experimental points are fitted with the log-normal model.

**3. Fundamental parameters.** Table I gives the chromatic dependence and the characteristic values, in the visible and the near infrared, of the fundamental parameters describing the image. Three essential, wavelength dependent, parameters will control the signal-to-noise ratio :

- (i) the maximum spectral bandwidth,
- (ii) the speckle lifetime, which determine the maximum exposure time in each image (see Roddier and Roddier, 1975);
- (iii) the Fried parameter  $r_0$ .

The Fried parameter plays a central role in speckle interferometry as, in the slit scanning system, the signal-to-noise ratio varies as  $r_0^4$ .

Parameter		Chromatic dependence	Charateristic value as a function of the wavelength ( $\mu\text{m}$ )			
			0.5	2.19	3.61	4.64
Fried parameter	$r_0$ (cm)	$\lambda^{6/5}$	10	50	110	145
Seeing angle ( $1.27\lambda/r_0$ )	$\omega$ (")	$\lambda^{-1/5}$	1.3	1.	0.9	0.8
Number of speckles (D=3.6m)	$N_s$	$\lambda^{-12/5}$	3000	80	25	14
Speckle lifetime	$\tau_s$ (ms)	$\lambda^{6/5}$	10	60	110	145
Isoplanatic angle	$\theta$ (")	$\lambda^{6/5}$	$\approx 4$ (1)	$\sim 40$ (2)		
Maximum spectral bandwidth	$\Delta\lambda$ (Å)	$\lambda^2$	100	Atmospheric windows		

Table I

(1) Roddier (1981) p.324  
 (2) Measured value

### III-THE INFRARED CASE

1. The slit system. Up-to-now all the infrared speckle results have been obtained with one dimensional systems using a single detector and a slit - of width  $\sim \lambda/D$  - on which the image is swept, in order to obtain the object power spectrum in the scan direction. As an example the specklograph of the ESO 3.6m telescope (figure 2) is attached to the Cassegrain adaptor, this configuration enables the whole system to be rotated along the optical axis and thus to explore various directions of the object. It makes use of the standard ESO infrared photometer/spectrophotometer equipped with a solid nitrogen cooled ( $\sim 50K$ ) InSb detector operating in photovoltaic mode (Moorwood, 1982). The image sweeping is achieved by means of a saw-tooth driven oscillating mirror controlled in frequency and amplitude (see Perrier, 1981, 1982, Léna, 1981).

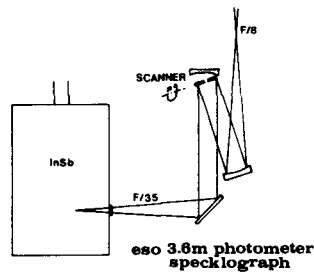


Fig.2. The specklograph installed at the Cassegrain focus of the ESO 3.6m telescope.

(After Léna, 1981)

2. The noise . In the near infrared we are not limited by the photon noise from the source but by an additive noise independent of the signal. For an optimized specklograph, the Johnson noise of the detector feedback resistor dominates at  $2.2\mu m$ , and the photon noise from the background dominates at longer wavelengths (see Moorwood, 1983). In practice this noise is estimated near the object by making the scans twice as long as the image (figure 3).

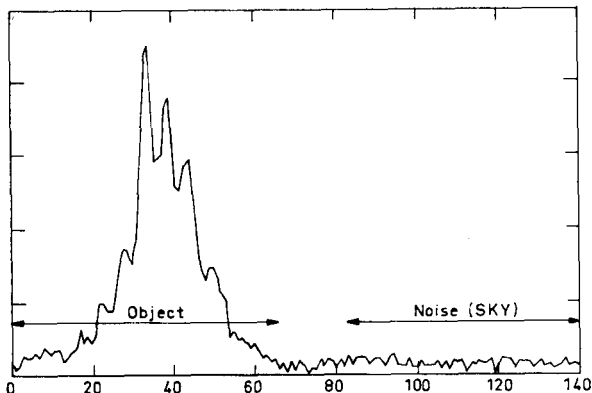


Fig.3. A typical scan pattern after sampling.  
(After Sibille et al., 1979)

3. The object power spectrum. Let  $i(\alpha)$  be the signal on the object part and  $b(\alpha)$  the signal on the sky part, the image power spectrum  $\langle |\tilde{I}(u)|^2 \rangle$  is given by

$$\langle |\tilde{I}(u)|^2 \rangle = \langle |\tilde{i}(u)|^2 \rangle - \langle |\tilde{b}(u)|^2 \rangle + c$$

where  $c$  is a cross-term which converges to zero when a large number of scans are averaged.

In the ideal case, if the seeing conditions are stable, the object power spectrum is obtained by dividing the image power spectrum with the speckle transfer function determined on a reference point source as close as possible to the object

$$|\tilde{O}(u)|^2 = \frac{\langle |\tilde{i}(u)|^2 \rangle_o - \langle |\tilde{b}(u)|^2 \rangle}{\langle |\tilde{i}(u)|^2 \rangle_r - \langle |\tilde{b}(u)|^2 \rangle}$$

the indices  $o$  and  $r$  referring respectively to the object and the reference (see figures 4a and b).

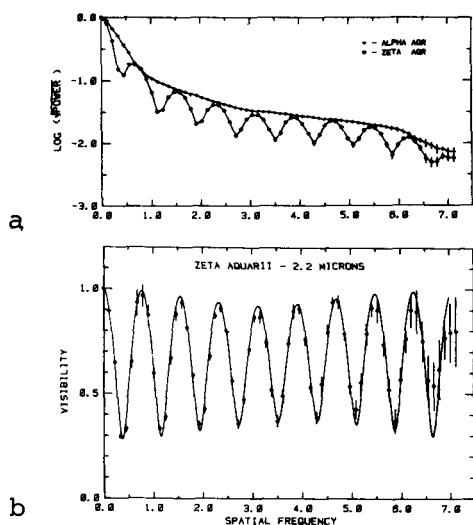


Fig.4 a) Spatial frequency spectra of  $\alpha$  Aqr, the speckle transfer function, and  $\zeta$  Aqr at  $2.2\mu\text{m}$ .

b) Visibility of  $\zeta$  Aqr at  $2.2\mu\text{m}$ . (After McCarthy et al., 1982a)

In practice the situation is much more complicated because the speckle transfer function depends on the Fried parameter  $r_0$  which is generally varying with time. If we do not have a system which gives a measure of  $r_0$  in real time to calibrate the observations, the faintest observable sources will be those for the signal-to-noise ratio is high enough in a few minutes integration time - during that time  $r_0$  is not supposed to vary too much. The source spectrum is considered to be correct if it is reproducible.

4. Instantaneous limiting magnitudes. The signal-to-noise ratio in infrared speckle interferometry has been computed by Sibille et al. (1979). For  $M$  statistically independent images, it is given by

$$\frac{S}{N} = \frac{\langle |\hat{I}(u)|^2 \rangle}{\langle |\hat{I}(u)|^2 \rangle + \langle |\hat{b}(u)|^2 \rangle} M^{1/2}$$

We will define the instantaneous limiting magnitudes by

$$R = \frac{\langle |\hat{I}(u)|^2 \rangle}{\langle |\hat{b}(u)|^2 \rangle} = 1$$

namely the signal is equal to the noise for one image. For such sources,  $S/N$  is equal to

$$\frac{S}{N} = \left( \frac{M}{4} \right)^{1/2}$$

A few hundred scans (or a few minutes integration time) will be sufficient to insure a good  $S/N$ .  $R$  can be expressed in function of the photon flux  $N$  from the source, the slit width  $\ell$ , the scantime  $\tau$ , the Fried parameter and the telescope diameter

$$R \propto N^2 \ell^2 r_0^4 \tau \quad \text{at } 2.2 \mu\text{m}$$

$$R \propto \frac{N^2 r_0^4 \tau}{D} \quad \text{at } 3.6 \text{ and } 4.6 \mu\text{m}$$

We see that if there are speckles in the image,  $R$  - or  $S/N$  for faint sources ( $R < 1$ ) - is proportional to  $r_0^4$ , is independent of the telescope diameter at  $2.2 \mu\text{m}$  and decreases with it a longer wavelengths. Table II gives (i) the instantaneous limiting magnitudes, (ii) the magnitudes of the faintest observed sources, (iii), the last values corrected for the parameters used to compute the instantaneous limiting magnitudes, (iv) the instantaneous limiting magnitudes for diffraction limited observations.

At  $2.2$  and  $3.6 \mu\text{m}$  there is a good agreement between theoretical and experimental limiting magnitudes (Table II, lines 1 and 3), at these wavelengths the speckle systems have achieved their limiting sensitivity. This is not the case at  $4.6 \mu\text{m}$ , the 1.5 magnitudes difference are probably due to an additional noise related to the fluctuations of the atmospheric emissivity as already suggested by Perrier (1982). Non published measurements made at UKIRT show that at  $5 \mu\text{m}$  the noise of the atmospheric emission is 6 times larger than the theoretical one, which

corresponds to a loss of 1.9 magnitudes in sensitivity comparable to the former 1.5 magnitudes.

**Table II**  
Instantaneous limiting magnitudes

$\lambda$	2.19	3.61	4.64
IIM <sup>(1)</sup>	6.9	6.6	4.9
Faintest observed sources	8.3 <sup>(3)</sup>	4.9 <sup>(4)</sup>	3.7 <sup>(5)</sup>
Corrected $m_{\lambda}$ <sup>(2)</sup>	7.3	6.1	3.4 ?
IIM , diffraction limited	10.4	8.8	6.6

(1)  $R = 1$

Seeing angle : 1"3 at 0.5 $\mu$ m

Telescope diameter : 3.6m

Scan rate : 20"/s

(2) In the ESO photometric system, zero magnitudes correspond to 673, 269, 158Jy in the K,L,M bands ( Wamsteker,1981)

(3) NGC 1068; McCarthy et al., 1982b

(4) NGC 1068; Perrier and Chelli, 1984

AFGL 618; Dyck et al., 1984

(5) T Tauri; Dyck et al., 1982

5. Observing method . The adopted method is to estimate several independent power spectra of the object by alternating its observations with those of the reference point source in order to compensate the temporal seeing variations. In the ESO system the number of scans to record on each source, the amplifier gains and the respective coordinates are fetched to the computer before the observation. During the acquisition the telescope points automatically and alternately the object and the reference; data recording is done after centring . This procedure has the advantage to be very rapid, for the apparent coordinate differences are updated after each telescope movement, therefore the pointing is precise. For a few degrees distance and during 1 hour it is possible to obtain more than ten independent estimations of the power spectrum of a bright source ( $R_{\lambda} > 1$ ) . The latter is computed in real time and displayed after each object-reference sequence allowing to control the data quality. It is useful or even necessary to repeat the measurements under different observing conditions in order to avoid the power spectrum to be biased because of systematic seeing variations between the object and the reference.

## 6. Data processing.

**6.1. Speckle interferometry.** After the observations the independent power spectra are recalculated. If they are consistent, their dispersion determines the error on the final power spectrum, result of the reduction using the averages of data on the object and on the reference. The error can be reduced with an algorithm developed by Perrier (1982) where the object power spectrum is estimated by an iterative procedure using the low frequency asymptotic expression of the speckle transfer function (Fried, 1966). The power spectrum interpretation can be done by modelling the spatial intensity distribution in case of a priori knowledge of the physics of the source (Allen et al. 1981; Jiang et al., 1984). We can also fit the power spectrum with one or several functions: the fitting with Bessel or gaussian functions allows to estimate sizes down to 50% of the Airy disk size; however this process can introduce errors if the source has a complex geometry (see the detailed discussion by Dyck et al., 1984). It is possible to reconstruct the spatial profile of extended components ( $\sim \lambda/D$ ) of an object by means of appropriate algorithms (see section III).

**6.2. Imagery.** Imagery methods are applicable to speckle interferometry data and they essentially consist of image selection and/or recentring (Dyck and Staude, 1982; Mariotti et al., 1983). They are quite suitable when the Fried parameter is of the order of, or larger than 1 meter - as it is often the case in the near infrared, see Table I - namely comparable to the diameter of current large telescopes ( $D \sim 4$  m).

Image recentring is of special interest when it is not possible to apply classical speckle methods; it consists of a first order treatment, always preferable from the signal-to-noise ratio point of view, by averaging recentred images. This method has been applied to reconstruct the profile of the source IRC2 at  $4.64\mu\text{m}$  (Chelli et al., 1984; see figure 5). The recentring has been done with respect to the maximum of the bright source BN located  $9''$  apart and recorded at the same time than IRC2, not visible itself on one scan. During the observations the ratio  $D/r_0$  was equal to 3, which corresponds to the case where the correction for image motion is most efficient to reduce the total image spread as shown by Fried (1966).

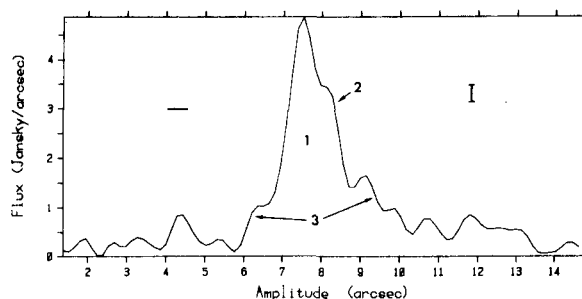


**Fig.5 .** Deconvolved spatial profile of IRC2 at  $4.64\mu\text{m}$  after image selection and recentring.

Image selection methods in the near infrared come from the "lucky short exposure concept" introduced by Fried (1978). Fried notes that the probability  $P$  of having an rms deviation less than 1 rad in the random phase introduced by the atmosphere over a pupil of diameter  $D$  is given by

$$P = 5.6 \exp\{-0.156 (D/r_0)^2\} \text{ valid for } D/r_0 > 3.5$$

If we admit that a diffraction limited image corresponds to 20% of maximum contrast loss or to a maximum phase deviation of 0.4 rad ( $\lambda/15$ ), we find using the generalized Fried formula (Cortegiani et al., 1981) that the probability to get such an image is

$$P = 11\% \text{ for } D/r_0 = 2$$

Figure 6 shows quasi-diffraction limited images on  $\eta$  Carinae and a reference point source obtained on the ESO 3.6m telescope. (Chelli et al., 1983).

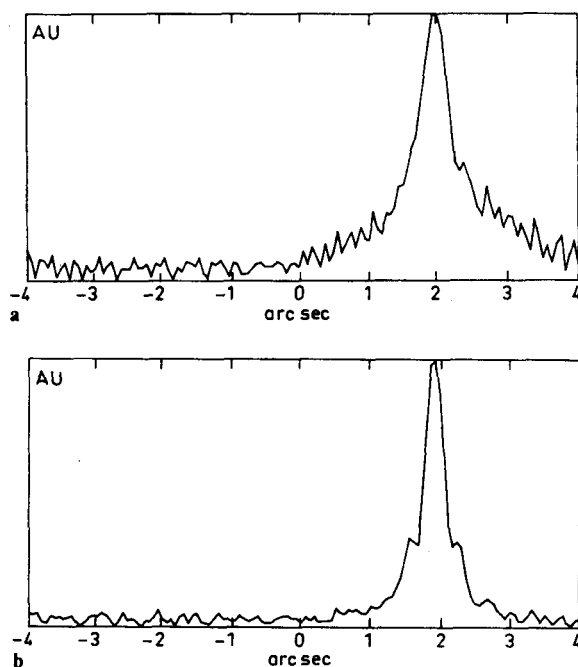


Fig.6. quasi-diffraction limited images. a)  $\eta$  Carinae, note the envelope around the source.

b) reference star, note the first diffraction ring seen through the slit.

In the same order of ideas, Mariotti (1983) has shown that, at least in some cases, the realisations  $r_e$  of  $r_0$  have a log-normal statistics of standard deviation  $r_0^2/D$ . Figure 7 gives the probability to get a diffraction limited image in function of the visible seeing; contrary to the visible domain where it is quasi-zero, this probability becomes important in the infrared from seeing angle less than 1".

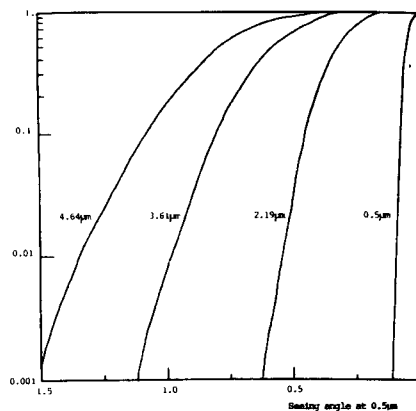


Fig.7. Probability to get a diffraction limited image in function of the visible seeing angle for a 3.6m telescope.

There are multiple advantages to work on diffraction limited images :

- (i) it is possible to observe very faint sources (see Table II, line 5),
- (ii) the object power spectra are obtained with a high precision, unaffected by seeing variations, hence the possibility to estimate very small sizes less than 50% of the Airy disk size,
- (iii) spectrum phase recovery can easily be done (see Chelli et al., 1983).

7. Infrared arrays. The considerable developments of infrared arrays (CID or CCD) bring new perspectives for ground and space astronomy. Some preliminary results (Sibille et al., 1982; Arens et al., 1983; Moneti et al., 1983) show that it will soon be possible to produce efficiently infrared images of the sky or to study systematically the high resolution bidimensional spatial structure of morphologically interesting objects.

Several parameters are useful to define an array (see Craig et al., 1982; McLean and Wade, 1983); we can mention :

- (i) observational level : format, size and pixel number, sensitivity domain
- (ii) performance level : dynamics, linearity, dark current, quantum efficiency, read-out noise.

One can anticipate that astronomers will soon have to their disposal systems with a high dynamics ( $> 10^7 e^-$ ), a good linearity, a low dark current ( $< 500 e^-/s$ ), a low read-out noise ( $< 1000 e^-$ ) and a quantum efficiency equivalent to that of a single detector.

For two dimensional infrared speckle interferometry the signal-to-noise ratio  $R$  on a single exposure (for faint sources, see II.4) has the following dependence :

$$R \propto (N D r_o \tau)^2 \quad \text{at } 2.2\mu\text{m}$$

$$R \propto (N D r_o)^2 \tau \quad \text{at } 3.6 \text{ and } 4.6\mu\text{m}$$

As in the slit system, we are limited by the system noise at  $2.2\mu\text{m}$  (read noise) and by the photon noise of the background at longer wavelengths. The instantaneous limiting magnitudes (for a visible seeing angle of  $1''.3$  and a 3.6 m telescope) are roughly the same than in the one dimensional case but as  $R$  is proportional to  $(Dr_o)^2$  instead of  $r_o^4$ , the sensitivity increases with the telescope surface.

#### IV-IMAGE RECONSTRUCTION

1. Status of the problem. The speckle interferometry technique allows to estimate the dimensions of an object, or its components, up to the limiting resolution of large telescopes. However the method does not permit to determine the departure from central symmetry, characterized by a non-zero phase in the object spectrum.

This part is devoted to methods of phase restitution from speckle data and to some image reconstruction methods. It is necessary to insist on the fundamentally different nature of these two problems. The question is - on one hand, to determine in a given frequency domain a well-defined quantity, the phase - on the other hand, to estimate a representation as close as possible to the object image from an incompletely known object spectrum.

2. Phase restitution. With an appropriate treatment it is possible to have access to the phase information contained in the speckles. Several methods - often improperly called image reconstruction methods - have been developed in the last decade and some of them have already been applied to astrophysical cases.

2.1. The Knox and Thompson method. Introduced by Knox and Thompson in 1974 this technique is based on the phase correlation which holds for two consecutive points -  $\hat{i}(u)$  and  $\hat{i}(u + \Delta u)$  - of the image spectrum, when their distance  $\Delta u$  is small compared to the width of the atmospheric transfer function ( $1/\omega$ ). The phase of the quantity  $\langle \hat{i}(u) \cdot \hat{i}^*(u + \Delta u) \rangle$  converges to the phase difference between  $\hat{i}(u)$  and  $\hat{i}(u + \Delta u)$  and the phase of the image spectrum can be reconstructed step by step.

The difficulty of the method lies in its recursive nature. In one dimension it is necessary to have a high signal-to-noise ratio on the gradient because errors accumulate. This disadvantage disappears in two dimensions where the constraints are stronger : it is possible to reduce the phase error on one point to the error of the phase gradient by the use of algorithms developed for the active optics (Hudgin, 1976). Recently Deron and Fontanella (1984) and Nisenson and Papaliolos (1984) have shown that, for bright sources ( $R > 1$ ), the error on the phase gradient was of the order of  $M^{-1/2}$  where  $M$  is the number of images.

The Knox and Thompson method has already been used to reconstruct sunspot images in the visible (Stachnik et al., 1977, 1984) and  $\eta$  Carinae images in the near infrared (Chelli et al., 1983). One can hope that recent noise analysis will incite astronomers to use this method which is the logical continuation of the speckle interferometry technique.

2.2. Speckle holography. Proposed by Liu and Lohmann (1973) and Bates et al. (1973), this method is applicable when there is a point source in the isoplanatic domain near the object at a distance larger than the seeing angle. It is easy to show that the signal autocorrelation contains a quantity from which the phase of the object spectrum can be estimated.

Speckle holography has been used with success in the visible by Weigelt (1978) on multiple systems. Its application to the infrared domain remains problematical in so far as the probability to find a point source in the isoplanatic domain near an interesting source is quasi-zero if one excludes molecular clouds, although one can be disturbed by the extended emission due to diffused light.

2.3. Lynds, Worden, Harvey method - shift and add. The two methods of this section are of the same nature. They are based on the idea that a speckle is a noisy representation of the diffraction limited image. Without considering detailed calculation, the problem for Lynds et al. (1976), Welter and Worden (1980), is to find the position and the intensity of the brightest speckles in each image to compute an average speckle. One of the difficulties of this procedure is the introduction of a diffuse background which is apparently not very easy to separate from the average speckle. In this sense the approach of Bates and Cady (1980) is clearer: they compute the average of images recentered by translation to the brightest speckle.

This kind of technique is restricted to a limited class of objects. The main difficulty resides in the localisation of the speckle center; the object has to be bright, not too extended ( $\sim \lambda/D$ ) and must not possess components of comparable intensity.

2.4. Speckle masking. Speckle masking has been proposed by Lohmann et al. (1983) and applied to multiple systems in the visible by Weigelt and Wirmitzer (1983). The aim is to compute the triple average product.

$$\langle \tilde{i}(u) \tilde{I}(u') \tilde{I}^*(u+u') \rangle$$

For an additive noise -  $i = I + b$ , as it is the case in the near infrared -, it is easy to deduce the quantity

$$\langle \tilde{I}(u) \tilde{I}(u') \tilde{I}^*(u+u') \rangle$$

As in the case of the Knox and Thompson method, the use of different displacements  $u'$  allows to reconstruct step by step the phase of the image spectrum.

2.5. Walker method. The method developed by Walker (1981a, 1981b, 1982) is based on the properties of the analytical continuation  $\tilde{O}(z)$  in the complex plane of the object spectrum  $\tilde{O}(u)$ . The knowledge of  $|\tilde{O}(u)|$  and of the complex

zeros ( $Z_i$ ) of  $\hat{O}(Z)$  allows to reconstruct  $\hat{O}(u)$  (Walther, 1963). Unfortunately we have only access to the analytic continuation of  $|\hat{O}(u)|$ , and it is not possible to distinguish between a zero  $Z_i$  and its complex conjugate  $Z_i^*$ ; for  $N$  complex zeros, there are  $2^N$  solutions for  $\hat{O}(u)$ . The original idea of Walker is the introduction of the spectrum modulus  $|\hat{O}'(u)|$  obtained from exponentially filtered images. Comparison between the zeros of the analytical continuations of  $|\hat{O}(u)|$  and  $|\hat{O}'(u)|$  allows to suppress the ambiguity ( $Z_i$  or  $Z_i^*$ ) and to reconstruct  $\hat{O}(u)$ .

The method of analytical continuations shows that there is only one spectrum  $\hat{O}(u)$  compatible with  $|\hat{O}(u)|$  and  $|\hat{O}'(u)|$ , but its use is not obvious as it is difficult to localise the zeros in the presence of noise. To settle this problem, Walker proposes to include the Fienup algorithm - which will be described later - to estimate  $\hat{O}(u)$  with a representation of the object image consistent with  $|\hat{O}(u)|$  and  $|\hat{O}'(u)|$ .

One of the apparent difficulties of the Walker method is related to its very nature, namely the introduction of an exponential filtering which will considerably increase the noise in the image edges. Nevertheless the method seems to be interesting because of its generality and does not suffer from the error accumulation encountered in the Knox and Thompson technique.

2.6. Future prospects. Astronomers have at their disposal several methods to reconstitute the spectrum phase and consequently to reconstruct the image of the objects they are studying in speckle interferometry. It is desirable to use two or more methods provided that they are essentially dissimilar. In particular, one should keep in mind the techniques developed by Knox and Thompson, and Walker, and possibly the speckle masking technique.

3. Image reconstruction. We know that in order to reconstruct the image of an object of extensions  $(L_x, L_y)$ , it is enough to know its Fourier spectrum on an infinite rectangular grid of the  $(u,v)$  plane. But we also know that no system is capable to yield this information. One or a group of telescopes is a low-pass spatial filter and there are often holes in the  $(u,v)$  plane coverage as in radioastronomy where moreover the sampling can quasi-never be done on a rectangular grid. The question is as follows: how to fill the holes in the Fourier spectrum in such a way to give the closest representation of the object image consistent with the resolution? The problem may seem unsolvable and it would indeed be so if astronomical images were not limited and especially positive. But even taking into account these constraints the solution is not unique in general and the situation is even worse due to the noise. To solve entirely the problem it is necessary to introduce additional hypothesis which are implicitly

and more or less clearly contained in the various algorithms.

One can divide image reconstruction methods into two classes (see Wells, 1980): linear and non-linear methods. The linear methods appeared first, the solution (output) is obtained as a linear combination of the input. This type of algorithm is very sensitive to the noise, produces oscillations in the image and cannot take into account its positivity.

The non-linear methods are less sensitive to the noise, can a priori take into account the positivity of the image and as a consequence are capable of super-resolution. The main difficulty is that there are very expensive in computing time.

We will describe four algorithms, three of which are non-linear.

3.1. CLEAN. The CLEAN method has been introduced to the astronomical community by Högbom (1974) and is extensively used in radioastronomy. CLEAN decomposes linearly the image and identifies it to a set of point sources superimposed to a noisy background. The method is well adapted if the brightness distribution contains only a few sources at well separated small regions, namely if the brightness distribution is essentially empty (Schwarz, 1978). It can take into account the limits of the image but not directly its positivity. Schwarz (1978) has shown that CLEAN is a least square fit of sine functions to the measured Fourier spectrum.

The problems of the algorithm are related to the non uniqueness of the solution - which depends on the gain loop, on the number of iterations and on the a priori supposed limits in the image - and to the existence of instabilities which can lead, on images of extended sources, to modulations at spatial frequencies corresponding to unsampled parts of the  $(u,v)$  plane (Cornwell, 1982).

3.2. The Biraud method. The BIRAUD method is the first non-linear algorithm which appeared in the literature. Biraud (1969) chooses to represent the image  $O(\alpha)$  by the square of a real function  $f(\alpha)$ . The object spectrum is given by

$$\tilde{O}(u) = \tilde{f}(u) * \tilde{f}(u)$$

Knowing the Fourier spectrum  $\tilde{O}(u)$  in the frequency domain  $\{0, u_c\}$ , the purpose is to construct a sequence of function  $\tilde{f}_n(u)$ , whose convolution product -  $\tilde{g}_n(u)$  - converges to  $\tilde{O}(u)$  in the domain  $\{0, u_c\}$ . Starting with a random hermitian distribution  $\tilde{f}_0(u)$ , each term of the sequence  $\tilde{f}_n(u)$  is obtained by adding to the preceding one an hermitian perturbation chosen to minimise the quantity

$$M_n = \frac{1}{u_c} \int_0^{u_c} |\tilde{O}(u) - \tilde{g}_n(u)|^2 du$$

The process is stopped when  $M_n$  is smaller than the noise. But it can happen that  $M_n$  converges to a value larger than the noise. It is then possible to

extrapolate the spectrum at frequencies larger than  $u_c$ , which is equivalent to increasing the resolution.

The Biraud method produces images with a good and even a super-resolution, which are in general reliable representations of the object but which do not always possess its actual smoothness (see figure 8c).

3.3. The Fienup method. The Fienup method (Fienup, 1978) based on a modified version of the Gerchberg and Saxton algorithm is well adapted when we only know the spectrum modulus  $|\hat{O}(u)|$ . Fienup constructs a sequence of images  $g_n(\alpha)$  and forces it to converge to a positive image, whose spectrum modulus is equal to  $|\hat{O}(u)|$  (this scheme is general and we can use all the a priori knowledge of the object).

As in the Biraud method, the result must not depend on the first element of the sequence, in particular the method is valid if it exists only one positive image whose spectrum modulus corresponds to the measured one. Bruck and Sodin (1979) have shown that contrary to the one dimensional case and apart from a  $180^\circ$  ambiguity, the solution is in general unique in two dimensions. It is possible to accelerate the process of convergence by choosing the first element of the sequence close to the result, this is the approach of Bates (1982) who determines the first element with a first estimation of the phase of the object spectrum from the spectrum modulus. It is worth noting that the Bates method of phase estimation shows independently of that of Bruck and Sodin the generally unique character of the solution in more than one dimension (Fright and Bates, 1982).

3.4. The Maximum entropy method (MEM). The maximum entropy method has been introduced by Burg (1967) developed in optics by Frieden (1972) and exposed in radioastronomy by Ables (1974). The basic idea comes from an analogy that may exist between a density of probability and a brightness distribution whose spectrum is only partially known. This analogy suggests to define the entropy  $E$  of an image which, for the most probable solution namely the one which contains the minimum of information, has to be maximum in a way consistent with the data. This approach has raised a lot of objections, all the more as there is not unanimity on the form of the entropy, the most employed being

$$E_1 = -\int O(\alpha) \text{Log} O(\alpha) d\alpha \quad \text{and} \quad E_2 = \int \text{Log} O(\alpha) d\alpha$$

Nityananda and Narayan (1982) have insisted on the difficulty to a priori associate a density of probability to a brightness distribution. The interesting approach of Komesaroff and Lerche (1979), Komesaroff et al. (1981) shows that the positivity constraints confines the first unmeasured point in the object spectrum (in one dimension) to a circle in the complex plane, MEM choosing the center of the circle. According to Nityananda and Narayan MEM is a form of model fitting,

$E_1$  and  $E_2$  being particular case of a whole family of entropies. In this scheme, the choice of an entropy function is just a means of incorporating a priori information into the reconstruction process.

In spite of all the criticisms that have been expressed in particular because of the probabilistic interpretation, we think that the last developments show that MEM is from the mathematical point of view the best understood method. The solutions have the interest to be positive, smooth and free of ringing (Figures 8d, 9).

Note applications in polarized light (Ponsonby, 1974),  $\gamma$  rays (Skilling et al. 1981), X rays (Willingale, 1981), visible (Frieden and Swindell, 1976), infrared (Chelli et al. 1983) or radio (Wernecke, 1977). A large part of the applications has been stimulated by the algorithm of Gull and Daniell (1978) simple to use and cheap in computing time.

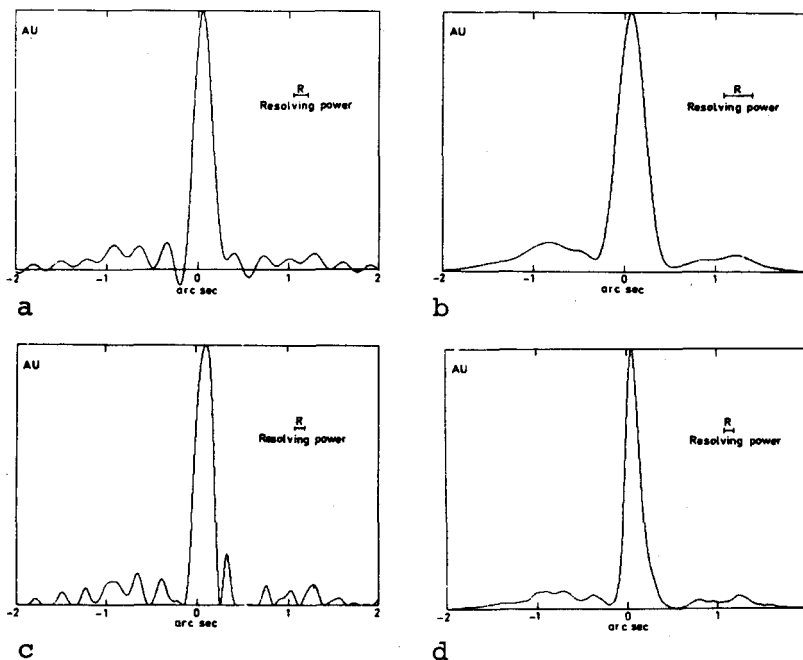


Fig.8. One dimensional high resolution image of  $\eta$  Carinae at  $4.64\mu\text{m}$   
 a) Principal solution  
 b) Apodized solution  
 c) Biraud solution  
 d) MEM solution

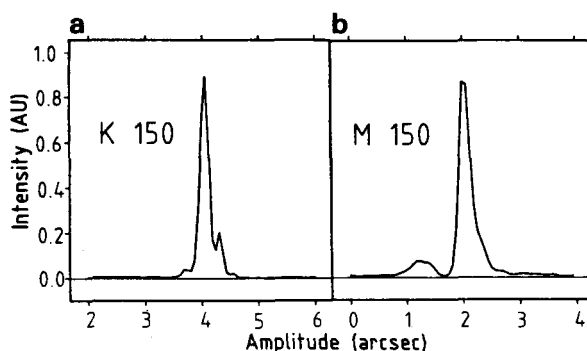


Fig.9. One dimensional high resolution image of  $\eta$  Carinae ( $\text{PA}=150^\circ$ )  
 a)  $2.2\mu\text{m}$   
 b)  $4.6\mu\text{m}$

3.5.Future prospects . Image reconstruction methods have progressed considerably during the last few years, especially owing to the introduction of non-linear algorithms less sensitive to noise than the linear ones and capable to take a priori into account the positivity of the image. Given the complexity of the problem and in the absence of a theory with which we can put error bars on the solution, we feel that it is necessary to compare the results of different methods. The most employed methods in the astronomical community are CLEAN and MEM, the last one seems to us potentially the most promising.

V-ASTROPHYSICAL APPLICATIONS . The spatial structure of an object depends on the physical phenomena which occur in it; it is an observational constraint that models have to reproduce. We have summarize in table III the results obtained for 6 years by speckle interferometry in the near infrared between 2 and 5 $\mu$ m. Except for the observations of the Seyfert galaxy NGC 1068 (McCarthy et al. , 1982b, Perrier and Chelli, 1984) and the astrometric applications relative to the discovery of infrared companions , see figure 10, (McCarthy et al., 1982a; Dyck et al., 1982; McCarthy, 1984), most of the measurements concern the circumstellar dust environment around very young (protostars ?) or on the contrary evolved stars (cool giant and supergiants, OH/IR sources, etc...).

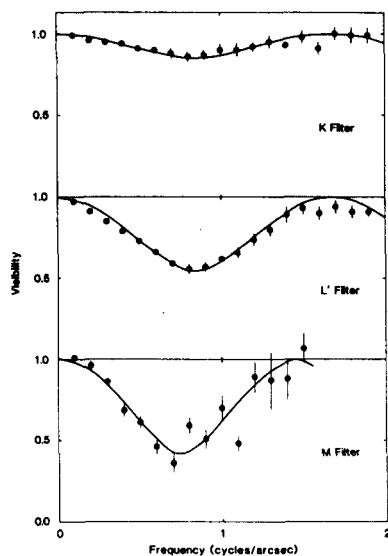


Fig.10. The double nature of T Tauri.

(After Dyck et al.,1982)

TABLE III

a) Protostellar candidates

Source	Distance (pc)	Luminosity (a) ( $10^3 L_{\odot}$ )	Angular dimensions (milliarc)	$\theta$ ( $\lambda$ , PA) (b)
KL - BN	480	10 - 20 <sup>(1)</sup>	$\lesssim 150$ (2.2, 90) <sup>(2)</sup>	$\lesssim 100$ (3.45, 40) <sup>(3)</sup> $\lesssim 80$ (4.8, 40) <sup>(3)</sup>
KL - IRC2	480	80 - 100 <sup>(4,5)</sup>	Complex structure (disk) $\approx$ $\lesssim 1400$ <sup>(c)</sup>	(4.64, 142) <sup>(4)</sup>
GL 490	900	1.4	$\lesssim 200$ (2.2, 90) <sup>(2)</sup>	
GL 989	800	4	$\lesssim 200$ (2.2, 90) <sup>(2)</sup>	$\lesssim 200$ (4.8, 0) <sup>(6)</sup>
CRL 2591	1500	40	$\lesssim 200$ (2.2, 0) <sup>(2)</sup>	$\lesssim 70$ (3.45, -) <sup>(7)</sup> $\lesssim 135$ (4.6, 33) <sup>(8)</sup>
NGC 2024 IRS2	500	10	$\approx 120$ (4.64, 90) <sup>(9)</sup>	
MonR2 IRS2	950	5	$\lesssim 200$ (4.8, 0) <sup>(2)</sup>	
MonR2 IRS3	950		Double : $\approx 870$ <sup>(d)</sup> (2.2 - 3.5 - 5, 13.5), $\lesssim 100$ <sup>(e)</sup> + halo : $\approx 2000$ <sup>(10,6)</sup>	
W3 IRS5	2300	200	Double : $\approx 1260$ <sup>(d)</sup> (5, 37), $\lesssim 250$ <sup>(e)</sup> (2, 6)	

b) Particular sources

Source	Distance (pc) <sup>(f)</sup>	Nature	Angular dimensions	$\theta$ ( $\lambda$ , PA) (b)
O Cet	40	Mira	$\lesssim 50$ (2.2, -) $\lesssim 100$ (3.45, -)	$\lesssim 100$ (4.8, -) <sup>(7)</sup> Variable diameter ?
$\eta$ Carinae	2800	O Type Supermassive object ( $\approx 160M_{\odot}$ )	Complex structure (disk?) + Image reconstruction	(2.2, 30 - 90 - 150) <sup>(11)</sup> , (4.64, 30 - 60 - 90 - 120 - 150) <sup>(11,12)</sup>
IRC+ 10216	290	Carbon star	Complex structure with a marked asymmetry at short wavelengths + non-resolved component $\lesssim 100$ emitting 20 to 30% of the flux <sup>(13,14,15,7)</sup> .	Observed in the CO fundamental rotation-vibration line at 4.7 $\mu$ m, size variation of a factor 3 relative to the spatial extension in the continuum <sup>(16)</sup> .
MMC 349	2100	-	$\lesssim 170$ (4.6, 90 - 150) <sup>(13)</sup>	
NGC 1068	$210^7$	Seyfert galaxy	Halo (600, Hubble law) + non-resolved component $\lesssim 200$ (2.2, 0) emitting 76% of the flux <sup>(17)</sup>	Double ? = $\approx 470$ <sup>(d)</sup> (3.6, $\approx 45$ ) <sup>(18)</sup>

Source	Distance (pc) <sup>(f)</sup>	Nature	Angular dimensions	$\theta$ ( $\lambda$ , PA) (b)
T Tauri	140	T Tauri	Double : $\approx 900$ <sup>(d)</sup> (2.2 - 3.8 - 4.8, $\approx 135$ )	$\lesssim 100$ <sup>(e)</sup> <sup>(21)</sup>
Ve 2 - 45	1900	WC9	$\approx 130$ (2.2, 0) = $\approx 250$ (3.8, 0) = $\approx 310$ (4.8, 0) <sup>(22, 23)</sup>	
Z Aquarii	23	Quadruple system	Detection of an infrared companion to Z Aquarii B <sup>(24)</sup>	
AFGL 618	1700	Bi-polar nebula	$\approx 130$ (3.8, -) <sup>(14)</sup>	
AFGL 915	330		Two components : $\approx 900$ (1.6 - 2.2 - 3.8 - 4.8, 0) + $\approx 80$ (2.2, 0) = $\approx 130$ (3.8, 0) = $\approx 160$ (4.8, 0) <sup>(14)</sup>	
OH 0739 - 14	2000		Two components : $\approx 2000 - 3000$ (3.8, 0 - 90) + $\approx 60$ (3.8, 0) = $\approx 40$ (3.8, 90) <sup>(14)</sup>	
M 2 - 9	1000		$\approx 110$ (3.8, 0) = $\approx 60$ (3.8, 90) <sup>(14)</sup>	
M 1 - 92	4500		$\approx 70$ (3.8, 0) = $\approx 50$ (3.8, 90) = $\approx 60$ (4.8, 90) <sup>(14)</sup>	

c) Giant and supergiants

Source	Distance (f) (pc)	Angular dimensions	$\theta$ ( $\lambda$ , PA) <sup>(b)</sup>
CIT 5	680	= <u>70</u> (4.8, 0) <sup>(14)</sup>	
CIT 6	190	= <u>60</u> (2.2, 0) = <u>80</u> (2.2, 90) = <u>100</u> (3.8, 0) = <u>140</u> (4.8, 0) <sup>(14)</sup>	
IRC+00365	-	$\zeta$ <u>170</u> (4.6, 90) <sup>(13)</sup>	
IRC+10420	3400	= <u>70</u> (2.2, 0) = <u>70</u> (2.2, 90) = <u>160</u> (3.8, 0) = <u>120</u> (3.8, 90) = <u>190</u> (4.8, 0) = <u>150</u> (4.8, 90) <sup>(14)</sup>	
IRC+20370	790	$\zeta$ <u>130</u> (4.6, 90) <sup>(13)</sup>	
NML Cyg	1800	= <u>80</u> (2.2, 0) = <u>140</u> (3.8, 0) = <u>190</u> (4.8, 0) = <u>150</u> (4.8, 90) <sup>(14)</sup>	
NML Tau	270	= <u>50</u> (3.8, 0) <sup>(14)</sup>	
OH 26.5 + 0.6	2200	Variable diameter ? (13, 14, 19)	
OH 308.9 + 0.1	-	$\zeta$ <u>100</u> (4.64, -) <sup>(20)</sup>	

Source	Distance (f) (pc)	Angular dimensions	$\theta$ ( $\lambda$ , PA) <sup>(b)</sup>
R Cas	-	$\zeta$ <u>100</u> (4.8, -) <sup>(3)</sup>	
R Leo	210	$\zeta$ <u>75</u> (2.38, 90) <sup>(13)</sup>	
SW Wlr	250	= <u>90</u> (2.38, 90) <sup>(13)</sup>	
U Her	310	$\zeta$ <u>100</u> (4.6, 150) <sup>(13)</sup>	
V Cyg	610	= <u>50</u> (3.8, 0) <sup>(14)</sup>	
VX Sgr	1500	= <u>50</u> (2.2, 0) = <u>100</u> (3.8, 0) <sup>(14)</sup>	
Cyg	97	= <u>100</u> (4.6, 90) <sup>(13)</sup> = <u>110</u> (4.8, 0) <sup>(14)</sup>	
VY CMa	1500	= <u>120</u> (3.8, 0) = <u>140</u> (4.8, 0) <sup>(14)</sup>	

- References : (1) Scoville et al., 1983. (2) Howell et al., 1981. (3) Chelli et al., 1979.  
 (4) Chelli et al., 1984. (5) Wynn-Williams et al., 1984. (6) Dyck and Howell, 1982.  
 (7) Foy et al., 1979. (8) Mariotti et al., 1983. (9) Jiang et al., 1984.  
 (10) McCarthy, 1982. (11) Perrier and Chelli, 1984a. (12) Chelli et al., 1983.  
 (13) Mariotti et al., 1983. (14) Dyck et al., 1984. (15) Selby et al., 1979.  
 (16) Dyck et al., 1983. (17) McCarthy et al., 1982b. (18) Perrier and Chelli, 1984.  
 (19) Perrier, 1983. (20) Perrier, 1982. (21) Dyck et al., 1982. (22) Allen et al., 1981.  
 (23) Dyck et al., 1984. (24) McCarthy et al., 1982a.

- (a) If not specified, the distance and the luminosity are taken from the compilation of Wynn-Williams (1982). Except for BN and IRC2 the luminosity refers to the entire molecular cloud.  
 (b) Equivalent uniform disk diameter or FWHM of gaussian profiles in the case of reference (14). The wavelength and the PA of observation are indicated in parentheses (PA = position angle counted counterclockwise with origin at the north).  
 (c) FWHM  
 (d) Separation, the PA is corresponding to the alignment of the sources.  
 (e) Refers to the individual sources.  
 (f) The distances are taken from the quoted papers.

1) Circumstellar envelopes. Protostellar sources and most of (if not all) evolved stars are surrounded by an envelope formed with a mixture of gas and dust whose characteristic dimension is of the order of  $2 \cdot 10^{15}$  cm, or  $0''.14$  at 1 Kpc distance, which roughly corresponds to the resolution of a 4m telescope in the near infrared.

(i) The energy distribution in the continuum depends on the characteristics of the envelope - optical properties of the dust grains, temperature, optical thickness, internal radius, or geometry - that high angular resolution observations allow to precise.

(ii) It is possible to have access to the material distribution near the star in the internal regions of the envelope by making measurements in the lines (Labeyrie, 1980; Dyck et al., 1983) - simultaneous observations in the continuum and in the lines allow to gain 2 to 3 magnitudes in sensitivity (Roddier, 1983) - , which contributes to clarify the mechanisms of excitation of the SiO maser lines and the molecular vibration-rotation lines such as CO ( see figure 11) and OH lines which need extreme physical conditions (high temperature, strong density)

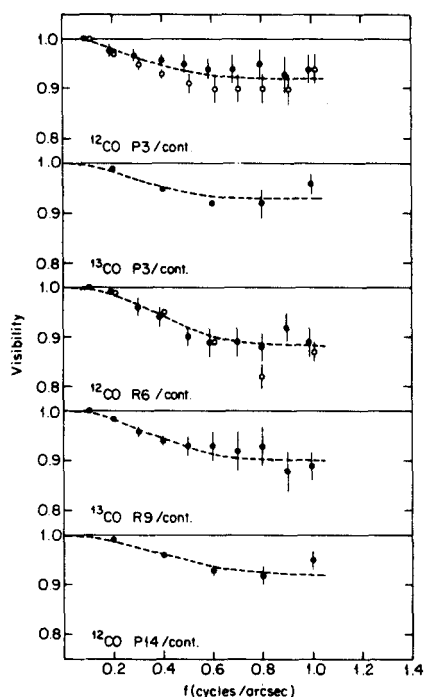


Fig.11. Visibility of 5 CO fundamental vibration-rotation lines relative to the visibility of a nearby continuum.

(After Dyck et al., 1983)

(iii) Other studies can be considered such as the follow-up of material movements in the internal part of the envelope of variable sources. For OH/IR sources which seem to be an extreme case of Mira type variables, correlations between the phase and the linear size will bring decisive clues to understanding their pulsation mode (see figure 12).

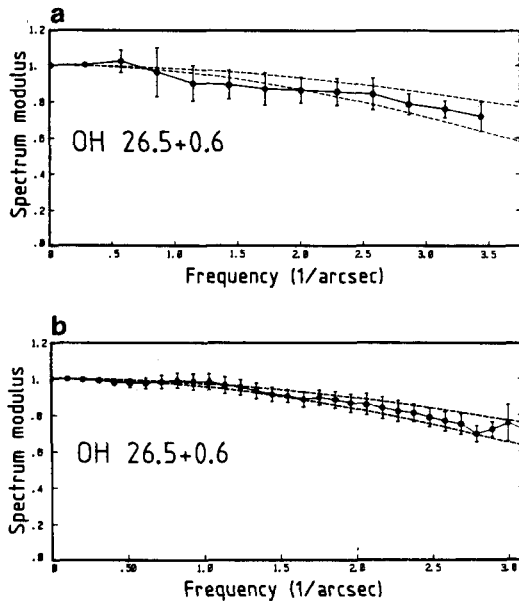


Fig.12. Visibilities of  
OH 26.5 + 0.6 at 4.64 $\mu$ m

a) June 1981 (0".14  $\pm$  0.02)

b) April 1982 (0".17  $\pm$  0.02)

(After Perrier, 1983)

(iv) Generally, a statistical analysis of the morphology and the extension of a large number of objects of similar nature allows to have access to the representative characteristics of a given class of objects beyond their individual peculiarities (see Dyck et al., 1984).

2) "Protostellar" sources. We do not know very well what is the precise sequence of events which take place during the formation of a star and many questions such as those concerning the momentum transfer from the primitive cloud to the newly formed star or the role of the magnetic field, have not satisfactory answers yet. For a spherical cloud one generally admits (see Yorke, 1981) that after an isothermal collapse phase, a small dense optically thick condensation forms, evolving slowly towards the main sequence while still accreting material. For low mass ( $M < 3 M_{\odot}$ ) "protostars" the core becomes visible before reaching the main sequence, this stage being observationally identified to T Tauri and YY Orionis objects. For the more massive protostellar clouds ( $M > 3 M_{\odot}$ ), the "protostar" will reach and spend part of its life on the main sequence still accreting material and completely obscured in the visible. It is justified to wonder whether it is possible to identify the last case to the sources of table IIIa, for they are objects :

(i) probably very young, associated to molecular clouds showing signs of recent star formation (proximity of OB associations, compact HII regions, intense CO emission, H<sub>2</sub>O, OH masers etc...), (ii) massive ( $M > 3 M_{\odot}$ ), with a high luminosity ( $L > 10^3 L_{\odot}$ ), (iii) completely obscured in the visible.

This identification raises some problems, for example one has never observed accretion, but on the contrary mass-loss, often anisotropic, up to  $10^{-3} M_{\odot}/\text{yr}$ .

It seems that models, in particular those with a spherical geometry, give a very simplified qualitative picture of the formation of a star, and are far from reproducing a much more complex reality. Among the sources of table IIIa, two sources over nine - Mon R2 IRS 3 and W3 IRS 5 - are double at the scale 1000-3000 AU, two others - BN and NGC 2024 - are marginally resolved and can be identified to B0 - B0.5 ZAMS (Scoville et al. 1982; Jiang et al., 1984). The only entirely resolved object is IRC2 from the KL nebula in OMC1. Its size of  $1''.4$  (700 AU) leads to a luminosity of  $(8^{+5}_{-3}) 10^4 L_{\odot}$  (Chelli et al., 1984) comparable to the  $10^5 L_{\odot}$  proposed by Wynn-Williams et al. (1984), which confirms that IRC2 is the main heating source in OMC1 (Downes et al., 1981). Its spatial profile at  $5\mu\text{m}$  is consistent with the disk structure (see figure 13) explaining well the 86 GHz SO emission (Plambeck et al., 1982) and the SiO maser polarization (Barvainis, 1984). Infrared, millimetric and radio data show that

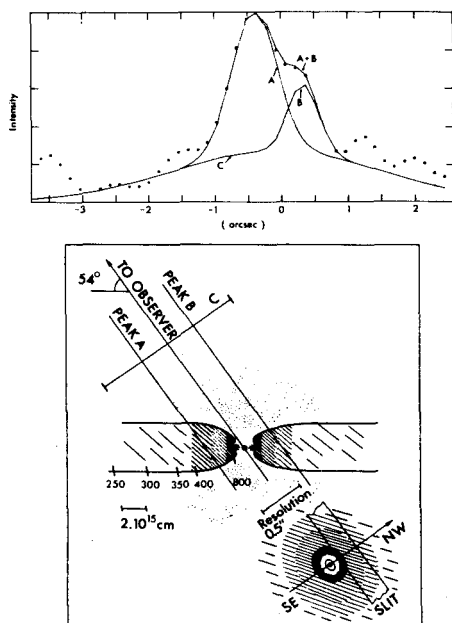


**Fig.13.** At the top, the double central core of IRC2 at  $4.64\mu\text{m}$  (dots). At the bottom, a proposed disk model. (After Chelli et al., 1984)

the disk is perpendicular to the high velocity ( $\sim 100\text{km/s}$ ) bipolar outflow observed in CO lines (Erickson et al., 1982), the origin of which is probably IRC2 (Wright et al., 1983). Other disks have been observed in radio around young sources such as S106 (Bally et Scoville, 1983) or NGC 2071 (Bally, 1982). It will be interesting to see if there is a close correlation between this type of structure and the bipolar flows which seem to be a general phenomenon associated with, even if not particular to, young objects (Bally and Lada, 1983). A study in the near infrared of the spatial structure - at least in two directions and at several wavelengths - will contribute to clarify these points and will put severe constraints on the mechanisms of the flow formation which are not yet well understood.

3) Seyfert nuclei. One of the questions raised by the nucleus of Seyfert galaxies is related to the nature (thermal and/or non thermal) of their infrared emission. In the case of the type 2 Seyfert galaxy NGC 1068 it seems that the infrared emission has a thermal origin (see Rieke and Lebofsky, 1979). NGC 1068 is the only extragalactic object observed by infrared speckle interferometry. The model of Jones et al. (1977) predicts a minimum extension of 0".8 consistent with the estimation of Becklin et al. (1973) at 10 $\mu$ m, but not consistent with those of Meaburn et al. (1982) in the continuum at 0.56 $\mu$ m -  $\sim$ 0".03 - and of McCarthy et al. (1982b) at 2.2 $\mu$ m -  $\sim$  0".2 - . At 3.6 $\mu$ m the measurements reveal a complex structure (Perrier and Chelli, 1984), possibly double at a 0".5 scale, lengthened in the radio jet direction, that we can compare with the triple structure coinciding with the nucleus and detected at 2cm (Van der Hulst et al., 1982; Wilson and Ulvestad, 1983). High spatial resolution observations allow to identify and to precise the geometry and the extension (at a 0".1 scale) of the infrared emitting regions, which are very important ingredients of the models. A large number of Seyfert galaxies has L magnitudes in the range 8-9 and their observation by speckle interferometry requires in practice diffraction limited images (see figure 14).

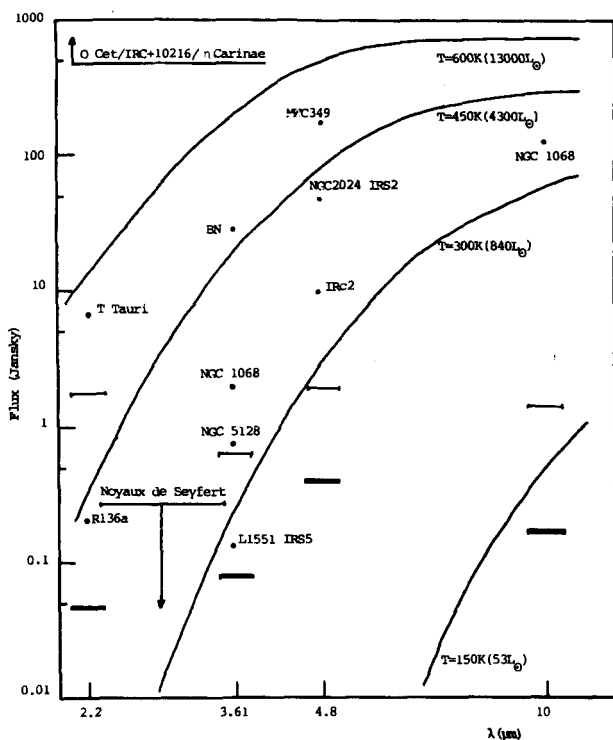


Fig.14. Heavy curves : infrared flux of a black body of 0".1 angular diameter, the corresponding luminosity at a 1 Kpc distance is indicated.

Horizontal bars : instantaneous limiting magnitudes for a 1".3 visible seeing angle and diffraction limited observations.

4) Future prospects. Only one "protostellar" candidate (IRC2) is entirely resolved, one Seyfert nucleus has been observed (NGC 1068) and the visibilities of evolved objects from Dyck et al. (1984) allow 50 to 80% of the flux to come from an unresolved component. In order that infrared speckle interferometry can keep its promises, in particular with respect to the statistical analysis important for the modelisation, one needs (i) a larger number of observations, (ii) a higher resolution, (iii) a better sensitivity.

A higher resolution can be achieved with larger telescopes, a 10 to 16m telescope would allow to resolve structures at a  $0.025''$  scale. In this scheme, an extension of the speckle interferometry method at  $10\mu\text{m}$  is interesting for the study of cool ( $T \sim 150\text{K}$ ) "protostellar" objects, which have a low luminosity ( $L \sim 50 L_{\odot}$ ) or which are in a not too advanced evolutionary stage.

A better sensitivity can only be achieved with very good seeing conditions, the importance of which is to be emphasised. With quasi-diffraction limited images it becomes possible to study the spatial structure of a large number of Seyfert nuclei. Other objects such as the infrared companion of T Tauri which might be a protoplanet (Hanson et al., 1983), MWC 349 interpreted as a protoplanetary disk (Thompson et al., 1977) or the individual components of multiple sources (NGC 1068 ?) need a higher resolution ( $< 0.01''$ ). This is the domain of infrared long baseline interferometry which has already proven its feasibility (Di Benedetto and Conti, 1982; Roddier and Léna, 1984).

VI-SUMMARY. The specific observing and data processing methods of near infrared speckle interferometry are now well understood. Though the systems have reached their limiting sensitivity, significant advance is expected from the follow-up of  $r_0$  in real time, which will allow to reduce the error bars on the final power spectra and make easier the observation of faint sources.

The considerable development of infrared arrays bring new perspectives for the speckle interferometry technique. It will soon be possible to efficiently produce high resolution bidimensional spectra of morphologically interesting objects. Astronomers have to their disposal several techniques with which they can reconstitute the phase of the spatial spectra and some of them have already produced results; the most promising to mention being the method of Knox and Thompson and the method of Walker. The techniques of image reconstruction raise more problems in reason of the absence of a theory allowing to put error bars on the solution, non linear methods and in particular the maximum entropy method seem to be the most interesting. From the astrophysical point of view infrared speckle interferometry is well adapted to the study of the circumstellar dust environment around very young or on the contrary evolved objects, or to the discovery of infrared companions.

Statistical analysis of the extension and the morphology of a large number of objects of similar nature and high spatial resolution in the lines - with a two channels system - are two very useful approaches for the modelisation. But there is a need of a higher resolution and a better sensitivity which can be achieved with a 10 to 16m telescope located in a "good site".

#### Acknowledgement

I would like to thank P.Léna, J.M.Mariotti, C.Perrier and F.Sibille for many interesting discussions and suggestions.

#### REFERENCES

- ABLES, J.G., 1974, *Astron. & Astrophys. Suppl. Ser.* 15, 383.
- AIME, C., KADIRI, S., RICORT, G., RODDIER, C., and VERNIN, J. 1979, *Optica Acta* 26, 575.
- ALLEN, D.A., BARTON, J.R., and WALLACE, P.T., 1981, *MNRAS* 196, 797.
- ARENS, J.F., LAMB, G.M., and PECK, M.C., 1983, *Optical Eng.* 22, 267.
- BALLY, J., 1982, *Ap.J.* 261, 558.
- BALLY, J., and LADA, C.J., 1983, *Ap.J.* 265, 824.
- BALLY, J., and SCOVILLE, N., 1983, *Ap.J.* 265, 497.
- BARVAINIS, R., 1984, submitted to *Ap.J.*
- BATES, R.H.T., 1982, *Physics Reports* 90, 203.
- BATES, R.H.T., and CADY, F.M., 1980, *Opt. Com.* 32, 365.
- BATES, R.H.T., GOUGH, P.T., and NAPIER, P.J., 1973, *Astron. & Astrophys.* 22, 319.
- BECKEFS, J.M., 1982, *Optica Acta* 29, 361.
- BECKLIN, E.E., MATTHEWS, K., NEUGFBAUER, G., and WYNN-WILLIAMS, C.G., 1973, *Ap.J.* 186, L69.
- BIRAUD, Y.G., 1969, *Astron. & Astrophys.* 1, 124.
- BRUCK, Y.M., and SODIN, L.G., 1979, *Opt. Com.* , 30, 304.
- BURG, J.P., 1967, in 37<sup>th</sup> Annual Sociandy of Exploration Geophysicists Meanding, Oklahoma City.
- CHELLI, A., LFNA, P., RODDIER, C., RODDIER, F., and SIBILLE, F., 1979, *Optica Acta* 26, 583.
- CHELLI, A., LFNA, P., and SIBILLE, F., 1979, *Nature* 278, 143.
- CHELLI, A., PERRIER, C., and BIRAUD, Y.G., 1983, *Astron. & Astrophys.* 117, 199.

- CHELLI, A., PERRIER, C., and LENA, P., 1984, *Ap. J.* (in press).
- CORNWELL, T.J., 1982, *Proceeding of the NRAO - VLA Workshop, New Mexico.*
- CORTEGGIANI, J.P., GAY, J., and RABBIA, Y., 1981, in *ESO Conference on Scientific Importance of High Angular Resolution at Infrared and Optical Wavelengths, Proceeding, Garching*, p. 175 .
- CRAIG, R., Mc CREIGHT, C.R., and GOEBEL, J.H., 1982, *Proc. SPIE* 331, 20.
- DAINTY, J.C., 1973, *Opt. Com.* 7, 129.
- DERON, R., 1983, *Thèse de 3ème cycle, Université de Nice.*
- DERON, R., and FONTANELLA, J.C., 1984, *J. Optics* (in press).
- Di BENEDETTO, G., and CONTI, G., 1983, *Ap.J.* 268, 309.
- DOWNES, D., GENZEL, R., BECKLIN, F.E., and WYNN-WILLIAMS, C.G., 1981, *Ap.J.* 244, 869.
- DYCK, H.M., BECKWITH, S., and ZUCKERMAN, B., 1983, *Ap.J.* 271, L79.
- DYCK, H.M., and HOWELL, R.R., 1982, *A.J.* 87, 400.
- DYCK, H.M., SIMON, T., and ZUCKERMAN, B., 1982, *Ap.J.* 255, L103.
- DYCK, H.M., SIMON, T., and WOLSTENCROFT, R.O., 1984, *Ap.J.* (in press).
- DYCK, H.M., and STAUDE, H.J., 1982, *Astron. & Astrophys.* 109, 320.
- DYCK, H.M., ZUCKERMAN, B., LEINERT, C., and BECKWITH, S., 1984, submitted to *Ap.J.*
- ERICKSON, N., and al., 1982, *Ap.J.* 261, L103.
- FIENUP, J.R., 1978, *Opt. Letters* 3, 27.
- FOY, R., CHELLI, A., SIBILLE, F., and LENA, P., 1979, *Astron. & Astrophys.* 79, L5.
- FRIEDEN, B.R., 1972, *JOSA* 62, 511.
- FRIEDEN, B.R., et SWINDELL, W., 1976, *Science* 191, 1237.
- FRIED, D.L., 1965, *JOSA* 55, 1427.
- FRIED, D.L., 1966, *JOSA* 56, 1372.
- FRIED, D.L., 1978, *JOSA* 68, 1651.
- FRIGHT, W.R., and BATES, R.H.T., 1982, *Optik* 62, 219.
- GERCHBERG, R.W., and SAXTON, W.O., 1972, *Optik* 35, 237.
- GULL, S.F., and DANIELL, G.J., 1978, *Nature* 272, 686.
- HANSON, R.B., JONES, B.F., and LIN, D.N.C., 1983, *Ap.J.* 270, L27.
- HOGBOM, J.A., 1974, *Astron. & Astrophys. Suppl. Ser.* 15, 417.
- HOWELL, R.R., Mc CARTHY, D.W., and LOW, F.J., 1981, *Ap.J.* 252, L21.
- HUDGIN, R.N., 1976, *JOSA* 67, 3.
- HUFNAGEL, R.E., and STANLEY, N.R., 1964, *JOSA* 54, 52.
- JIANG, D.R., PERRIER, C., and LENA, P., 1984, *Astron. & Astrophys.* (in press).

- JONES, T.W., LEUNG, C.M., GOULD, R.J., and STEIN, W.A., 1977, *Ap.J.* 212, 52.
- KOMESAROFF, M.M., and LERCHE, I., 1979, in *Image Formation from Coherence Functions in Astronomy*. Ed. c. Van Schooneveld, D. Reidel, Dordrecht, p. 241.
- KOMESAROFF, M.M., NARAYAN, R., and NITYANANDA, R., 1981, *Astron. & Astrophys.* 93, 269.
- KNOX, K.T., and THOMPSON, B.J., 1974, *Ap.J.* 193, L45.
- KORFF, D., 1973, *JOSA* 63, 971.
- KORFF, D., DRYDEN, G., and MILLER, M.G., 1972, *Opt. Com.* 5, 187.
- LABEYRIE, A., 1970, *Astron. & Astrophys.* 6, 87.
- LABEYRIE, A., 1980, in "Optical and Infrared Telescope for the 1990's", *Proceeding of the KPNO Conference, Tucson Az.*
- LENA, P., 1977, in *Infrared Astronomy*, Setti, G., Gazio, G. ed. Reidel.
- LIU, C.Y.C., and LOHMANN, A.W., 1973, *Opt. Com.* 8, 372.
- LOHMANN, A.W., WEIGELT, G.P., and WIRNITZER, B., 1984, submitted to *Applied Optics*.
- LYNDS, C.R., WORDEN, S.P., and HARVEY, J.W., 1976, *Ap.J.* 207, 174.
- Mc CARTHY, D.W., 1982, *Ap.J.* 257, L93.
- Mc CARTHY, D.W., 1984, preprint.
- Mc CARTHY, D.W., LOW, F.J., KLEINMANN, S.G., and GILLETT, F.C., 1982a, *Ap.J.* 257, L7.
- Mc CARTHY, D.W., LOW, F.J., KLEINMANN, S.G., and ARGANBRIGHT, D.V., 1982b, *Ap.J.* 257, L75.
- Mc LEAN, I.S., and WADE, R., 1983, preprint.
- MARIOTTI, J.M., 1983, *Optica Acta*, 30, 831.
- MARIOTTI, J.M., CHELLI, A., FOY, R., LENA, P., SIBILLE, F., and TCHOUNTONOV, G., 1983, *Astron. & Astrophys.* 120, 237.
- MEABURN, J., MORGAN, B.L., VINE, H., PEDLAR, A., and SPENCER, R., 1982b, *Nature* 296, 331.
- MONETI, A., FORREST, W.J., PIPHER, J.L., and WOODWARD, C., 1983, *BAAS* 15, 683.
- MOORWOOD, A., 1982, *The Messenger* 25, 26.
- MOORWOOD, A., 1983, in *ESO's Very Large Telescopes*, Cargèse 16-19 May.
- NIENSON, P., and PAPALIOIOS, C., 1984, submitted to *Opt. Com.*
- NITYANANDA, R., and NARAYAN, R., 1982, *J. Astron. & Astrophys.* 3, 419.
- PERRIER, C., 1982, *Thèse de 3ème Cycle, Université Paris VII, France*.
- PERRIER, C., 1983, *The Messenger* 33, 16.
- PERRIER, C., and CHELLI, A., 1984a,b, in preparation.
- PLAMBECK, R.L. et al., 1982, *Ap.J.* 259, 617.
- PONSONBY, J.E.B., 1973, *MNRAS* 163, 369.

- RIEKE, G.H., and LEBOWSKY, M.J., 1979, A.R.A.A. 17, 477.
- RODDIER, C., and RODDIER, F., 1975, JOSA 65, 664.
- RODDIER, C., and RODDIER, F., 1983, Ap.J. 270, L23.
- RODDIER, F., 1975, in Digest of Technical Papers, Meeting on Imaging in Astronomy, Cambridge Mass., pp. The 6/1 - The 6/4.
- RODDIER, F., 1981, in Progress in Optics 19, 283.
- RODDIER, F., 1983, in ESO's Very Large Telescopes, Cargèse 16-19 May, 155.
- RODDIER, F., and LENA, P., 1984, J. Optics (in press).
- ROWAN-ROBINSON, M., and HARRIS, S., 1982, MNRAS 200, 197.
- SCHWARZ, U.J., 1978, Astron. & Astrophys. 65, 345.
- SCOVILLE, N., KLEINMANN, S.G., HALL, D.N.B., and RIDGWAY, S.T., 1983, Ap.J. 275, 201.
- SELBY, M.J., WADE, R., SANCHEZ-MAGRO, C., 1979, MNRAS. 187, 553.
- SIBILLE, F., CHELLI, A., and LENA, P., 1979, Astron. & Astrophys. 79, 315.
- SIBILLE, F., LENA, P., CHELLI, A., and STEFANOVITCH, D., 1982, SPIE 331, 26.
- SKILLING, J., STRONG, A.W., and BENNETT, K., 1979, MNRAS 187, 145.
- STACHNIK, R.V., NISENSEN, P., EHN, D.C., HUDSON, R.H., and SCHIRF, V.E., 1977, Nature 266, 149.
- STACHNIK, R.V., NISENSEN, P., and NOYES, R.W., 1984, Ap.J. (in press).
- THOMPSON, R.I., STRITTMATER, P.A., ERICKSON, E.F., WITTEBORN, F.C., and STRECKER, D.W., 1977, Ap.J. 218, 170.
- van der HULST, J.M., HUMMEL, E., and DICKEY, J.M., 1982, Ap.J. 261, L59.
- WALKER, J.G., 1981a, Optica Acta 28, 735.
- WALKER, J.G., 1981b, Optica Acta 28, 1017.
- WALKER, J.G., 1982, Applied Optics 21, 3132.
- WALTHER, A., 1963, Optica Acta 10, 41.
- WEIGELT, G.P., 1978, Applied Optics 17, 2660.
- WEIGELT, G.P., and WIRNITZER, B., 1983, Optics Letters 8, 389.
- WELLS, D.C., 1980, SPIE 264, 148.
- WELTER, G.L., and WORDEN, S.P., 1980, Ap.J. 242, 673.
- WERNECKE, S.J., 1977, Radio Science 12, 831.
- WILLINGALE, R., 1981, MNRAS 194, 359.
- WILSON, A.S., and ULVESTAD, J.S., 1983, Ap.J., 275, 8.
- WRIGHT, M.C., PLAMBECK, R.L., VOGEL, S.L., HO, P.T.P., and WELCH, W.J., 1983, Ap.J. 267, L41.
- WYNN-WILLIAMS, C.G., 1982, A.R.A.A. 20, 587.
- WYNN-WILLIAMS, C.G., GENZEL, R., BECKLIN, E.E., DOWNES, D., 1984, Ap.J. (in press).
- YORKE, H.W., 1981, in ESO Conference on Scientific Importance of High Angular Resolution at Infrared and Optical Wavelengths, Proceeding, Garching, p. 319.